

A review of the implications of computational fluid dynamic studies on nasal airflow and physiology*

S.C. Leong¹, X.B. Chen², H.P. Lee², D.Y. Wang³

¹ Common Cold Centre and Healthcare Clinical Trials, Cardiff School of Biosciences, Cardiff University, Wales, United Kingdom

² Department of Mechanical Engineering, National University of Singapore

³ Department of Otolaryngology – Head and neck Surgery, Yong Loo Lin School of Medicine, National University of Singapore

SUMMARY

Background: Computational fluid dynamics has been adapted to studying nasal aerodynamics.

Aim: To review current literature on CFD studies, with an emphasis on normal nasal airflow, the impact of sinonasal pathology on airflow, and implications on nasal physiology. The objective is to provide the rhinologists with a greater understanding of nasal airflow and how symptomatology of sinonasal disease may be explained via CFD simulations.

Results: The nasal valve region redirects inspiratory airstreams over the inferior turbinate in a high turbulent kinetic energy, which is important in heat and moisture exchange. The bulk of airflow occurs in the common meatus with small streams traversing the olfactory groove, increasing during sniffing. Septal deviation and enlarged inferior turbinate causes redistribution of airflow, changes in intranasal pressure and increased turbulence. High velocity airflow and wall shear stress at the septal perforation causes desiccation and mucosal damage. The airflow within an atrophic nasal cavity is predominantly laminar with minimal contact with nasal mucosa. The inferior turbinate is an important organ for air conditioning and preservation during surgery is highlighted.

Conclusions: Despite some limitations of CFD simulations, this technology has improved understanding of the complex nasal anatomy and the implications of disease and surgery on physiology.

Key words: paranasal sinuses, physiology, computational fluid dynamics, airflow

INTRODUCTION

Computational fluid dynamics (CFD) is one of the branches of fluid mechanics that uses numerical methods and algorithms to solve and analyze problems that involve fluid flows. Computers are used to perform the calculations required to simulate the interaction of liquids and gases with surfaces defined by boundary conditions. A small but growing number of rhinology research centres have adapted CFD technology to study nasal airflow, physiology and to simulate outcomes following surgical intervention. It may be feasible in the near future to simulate the disordered nasal aerodynamics before performing a surgical procedure in every patient, thereby increasing the effectiveness of surgical planning and ultimately patient outcome⁽¹⁾.

Unlike previous review articles, which have focused on the technical aspects of CFD and the validity of using this technique in simulating nasal airflow^(2,3), this article focuses on the clinical relevance of CFD studies in understanding normal nasal physiology and the changes attributed to disease. We will

attempt to provide a comprehensive review of current literature on CFD studies, with an emphasis on normal nasal airflow, the impact of sinonasal pathology on nasal airflow and implications on nasal physiology. The objective is to provide the rhinologists with a greater understanding of nasal airflow and how symptomatology of sinonasal disease may be explained via CFD models. This article will also consider how surgical intervention may restore normal nasal aerodynamics.

The studies reviewed were obtained from a structured search of the U.S National Library of Medicine (PubMed) online database using a combination of MeSH terms (nose, paranasal sinuses) and non-MeSH terms (computational fluid dynamics, numerical simulation, airflow simulation). Studies focusing on nasal spray delivery and particle deposition using CFD models will not be considered as this topic has been previously reviewed⁽⁴⁾. The shortcomings of CFD in clinical studies will also be discussed.

NORMAL NASAL AIRFLOW

Unlike other methods of evaluating nasal airflow such as rhinomanometry and Mink box simulations, CFD offers an accurate and highly graphical model to better understand the nature of nasal airflow. The complex correlations between temperature and humidity, and how these variables affect aerodynamics can also be evaluated. Computational fluid dynamics offer a single evaluative modality that allows both sinonasal anatomy and physiology to be studied concurrently.

Previous studies have attempted to visualize the nasal valve region using endoscopy⁽⁵⁾, acoustic rhinometry and computer tomography⁽⁶⁾, but none have been able to illustrate the relationship between form (anatomy) and function (physiology) as in CFD. Simulations from 23 healthy volunteers showed that the nasal resistance in the area of 3cm distance from the nostril accounted for 52.6% to 78.3% of the total nasal airway resistance⁽⁷⁾. The results corroborated with earlier studies by Haight and Cole⁽⁸⁾ who, using a “head-out” body plethysmograph technique, reported that two-thirds of total nasal resistance was at the nasal valve region. In a review of the literature, Eccles reported that there was some dispute as to whether the nasal valve lied in the nasal vestibule or more posteriorly within the bony cavum of the nose⁽⁹⁾. However, the anatomical and physiological evidence at the time indicated that the nasal valve occurred at the entrance of the piriform aperture, with the major site of nasal resistance just anterior to the tip of the inferior turbinate. The boundaries of the nasal valve region included the caudal end of the upper lateral cartilage, the head of the inferior turbinate, the caudal septum, and the remaining tissues surrounding the piriform aperture.

The nasal valve changes the direction of the inspiratory air streams as it enters the vestibule and directs the bulk of air-flow around the inferior turbinate (Figure 1A). Figure 1B shows the sagittal section of the nasal valve region demonstrating turbulent kinetic energy during inspiration. The aero-

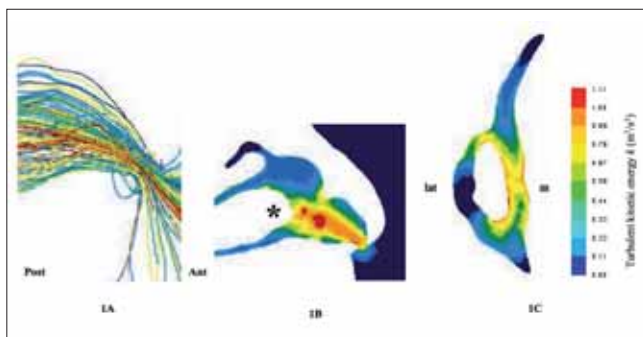


Figure 1. Computational fluid dynamic studies at the nasal valve region. 1A is the inspiratory airstreams at a flow rate of 17.5 L/min entering the nasal vestibule toward the nasal valve region), Ant = anterior, Post = posterior. 1B is the contour of turbulent kinetic energy κ (m^2/s^2) at a sagittal cross section during inspiration. * = inferior turbinate. 1C is at coronal cross section. m = medial, lat = lateral.

dynamics of the airflow altered significantly from a relatively laminar profile at the nasal vestibule to having high turbulent kinetic energy at the area anterior to the head of the inferior turbinate. When the air flowed around the inferior turbinate (Figure 1C), the airflow became less turbulent on the medial surface of the turbinate. This is important as contact with nasal mucosa facilitates heating/cooling and humidification of inspired air. Heat transfer from nasal mucosa to inspired air was shown to be concentrated in the Little’s area, the lateral wall of the vestibule, the inferior border of the middle turbinate and the anterior half of the inferior turbinate⁽¹⁰⁾. Conversely, distortion of the nasal valve region redirects inspired air streams superiorly into the middle meatus⁽¹¹⁾ and high turbulent energy causes increased wall shear stress, predisposing to mucosal damage. This may explain the symptoms of dryness and obstruction in cases of nasal valve collapse⁽¹²⁾.

Although individual variations occurred, the bulk of airflow passed through the common meatus with a smaller proportion flowing through the middle meatus^(7,13). This was also found in a CFD study by Xiong et al.⁽¹⁴⁾ that noted that airflow in the common and middle meatus accounted for over 50% and 30% respectively of the total nasal airflow. There was very little exchange between the paranasal sinus and the nasal cavity during normal quiet breathing but expectantly increased after endoscopic sinus surgery^(15,16). The act of sniffing encouraged the upper air streams of inspired air into the olfactory groove, which supported this manoeuvre whenever a person was presented with an olfactory stimulus⁽¹⁷⁾.

One of the main functions of the nose is the heating of inspired air before it reaches the lower respiratory tract. Conditioning of the respiratory air depends on both heating the air during inspiration and heat recovery during expiration, which is regained from the saturated and warmed expired air on the cooler mucosa. Water is preserved for humidification of the air during the following inspiration. The heat exchange

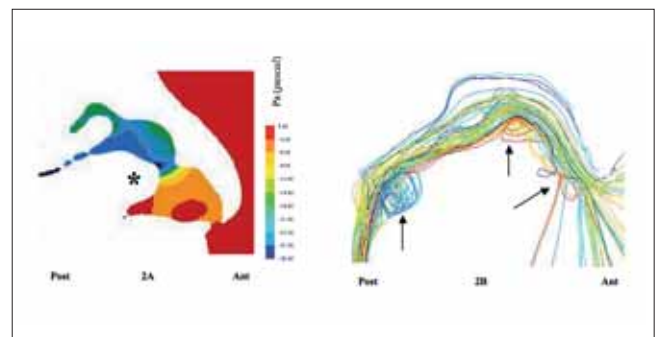


Figure 2. Effects of an enlarged inferior turbinate on nasal aerodynamics. 2A illustrates the changes in pressure contours during inspiration at the nasal valve region. Ant = anterior, Post = posterior, * = inferior turbinate. 2B is a sagittal view of streamlines. The arrows are areas of vortex flow.

function of the nose has been well demonstrated in a series of CFD studies by the Lindemann group⁽¹⁸⁻²⁰⁾. During inspiration, the greatest increase in air temperature occurred at the nasal valve region⁽¹⁸⁾. Progressively smaller temperature increments occurred distally and by the time the air stream had reached the nasopharynx, the temperature had risen to 33.9°C. Areas of high temperature increases, such as the nasal valve and head of inferior turbinate were associated with turbulent airflow with vortices of low velocity, indicating increased contact between air and mucosa. During expiration, the airflow medial to the inferior turbinate was turbulent with low velocity vortices where the greatest temperature decrease was also observed⁽¹⁹⁾. The inferior turbinates were the main region of heat exchange and complete resection reduces heating and humidification of inspired air⁽²⁰⁾.

ENLARGED INFERIOR TURBINATE

The nasal epithelium has a very complex vasculature with a submucosal plexus of venous sinuses lining the nasal mucosa. These venous sinuses form erectile tissue that is well developed in the anterior part of the nasal septum and the inferior turbinate, especially in the nasal valve region⁽²¹⁾. These submucosal cushions of venous sinuses expand and shrink, depending upon the degree of congestion, hence altering the caliber of the nasal passages and influencing the nasal airflow⁽²²⁾. The “head” of the congested turbinate extends proximally the nasal valve region to narrow, which results in increased resistance to nasal airflow. The cyclical congestion and decongestion of the turbinates is a physiological phenomenon of the nasal cycle.

However, pathological enlargement of the inferior turbinates is a common underlying mechanism of chronic nasal obstruction. The enlargement may be due to either the mucosal or osseous component, where the mean width has been reported to be nearly 11 mm when measured by computer tomography^(23,24). After MRI reconstruction of a healthy human subject, Lee et al.⁽²⁵⁾ simulated turbinate enlargement by expanding the inferior turbinate homogeneously outward by 1 mm and 2 mm to simulate moderate and severe nasal obstruction, respectively. Despite the small increment in the overall dimensions of the inferior turbinate, there was significant malfunction of the nasal valve resulting in increased total negative pressure in the nasal cavity during the inspiratory phase of breathing (Figure 2A). The velocity of nasal airflow reduced significantly around the head of the turbinate to 0.42 m/s, compared to 0.89 m/s in the normal healthy nose. Nasal airflow was redistributed toward the upper part of the nasal cavity at higher flow velocities causing increased wall shear stress at the olfactory zone (Figure 2B). It was postulated that the exaggerated fall in negative pressure in the nasopharynx due to the reduced flow rate could adversely affect the function of the surrounding muscles and mobility of the soft palate, which were common etiological factors for snoring and obstructive sleep apnea.

Given that the sensory receptors for airflow are located around the head of the inferior turbinate and anterior septal wall⁽²⁶⁾, the overall changes to normal nasal airflow caused by enlarged turbinates would explain the subjective complaint of nasal obstruction. Whether the changes in airflow pattern actually impair olfactory function remains to be answered. The higher flow velocity and lower pressure at the orifice of the Eustachian tube may actually cause abnormal function and lead to middle ear disorders.

Numerous surgical techniques have been described to treat turbinate enlargement, many of which were technology driven rather than evidence based⁽²⁷⁾. The low level evidence base for performing turbinate surgery is partly due to the lack of appropriate objective measures to assess surgical outcome⁽²⁸⁾. It should be noted that a return to normative rhinomanometric levels cannot be regarded as a return to normal airflow conditions, as rhinomanometry does not offer visualisation of actual streamlines and loco-regional pressure changes.

Three published studies have simulated intranasal airflow after virtual turbinate reduction in normal healthy subjects without any sinonasal complaints. Wexler et al.⁽²⁹⁾ reported a general reduction in intranasal pressure following resection of the medial surface of the inferior turbinate. The greatest reduction in pressure occurred at the nasal valve region. There was concomitant reduction in mean air velocities throughout the nasal cavity, especially in the posterior region. The bulk of the airflow was redistributed inferiorly along the floor of the nasal cavity. Similar observations were reported by Yu et al.⁽⁷⁾. In another study, Lindemann et al.⁽³⁰⁾ reported the adverse effects of middle and inferior turbinate resection on intranasal temperature. In their study, a large, elongated static vortex of air developed and due to the absent turbinates, the flow of air was generally laminar. The centre of the inspiratory air stream remained cool even when air had reached the nasopharyngeal region. The implications of this phenomenon on the lower airways and how it might predispose to pathology remain to be answered.

Given that surgery is normally indicated in chronic turbinate enlargement, it is unlikely that these models on normal subjects would approximate the aerodynamic consequences of surgery. Ideally, simulation studies of turbinate reduction procedures should be based on an enlarged turbinate model as the baseline, and then comparing the post-intervention aerodynamics with that of the normal nose. By demonstrating a return to near normal intranasal conditions, this would help clinicians decide which surgical technique to be most efficacious.

SEPTAL PERFORATION

Septal perforations are usually the result of self induced or iatrogenic trauma⁽³¹⁾. Although septal perforations are usually asymptomatic, it may present with significant symptoms such

as nasal obstruction, sensation of dryness, excessive crusting, epistaxis, whistling and headache⁽³²⁾. The nasal obstruction and whistling are related to abnormal aerodynamics, whilst the other symptoms are related to the poor condition of the nasal mucosa. Small perforations have a stronger tendency to produce sounds than larger ones, although the symptoms can be relatively mild.

Grützenmacher et al.^(33,34) were the first to study the effects of septal perforation on nasal airflow. The experiments were based on anatomically exact models of the nose in modified Mink boxes using both air and water. When CFD simulations were performed subsequently, Grant et al.⁽³⁵⁾ reported that the wall shear stresses were unevenly distributed in the septal perforation and was concentrated at the posterior edge of the perforation. As the area around the perforation is rich in blood vessels, this may explain the cause of epistaxis associated with this condition. However, the correlation between size of perforation and abnormal aerodynamics was not considered in this study, and it was also not known how large a perforation was simulated.

Pless et al.⁽³⁶⁾ simulated an anterior perforation in a reconstructed model taken from a healthy volunteer by removing an elliptical (horizontal diameter 20 mm, vertical 15 mm) shaped portion of the septum. Airflow patterns and air temperature distribution during inspiration were studied. Expectantly, intranasal conditioning of inspired air was abnormal. Due to the mixing of air from both nasal cavities, the air temperature was significantly lower than the normal nose. The shape of the central cooler air stream was larger around the perforation. The airflow traversing the perforation was at high velocity in a turbulent stream (Figure 3). Airflow velocities were observed to be highest along the posterior edge of the perforation, which corroborated with the findings of Grant et al.⁽³⁵⁾. The resulting increased wall shear stress caused mucosal desiccation and damage, which presents as epistaxis and crusting. Since a turbulent airflow provides more kinetic energy than laminar airflow, heat and water exchange between inspired air and nasal mucosa is more effective in areas of turbulence due to increased contact. An almost stationary vortex in the sagittal plane developing within the perforation was observed, which resulted in a prolonged and intensified contact between air and mucosa. This may cause irritation and desiccation of mucosa in the area of perforation. Noise may be produced when airflow velocity and turbulence exceeds a certain threshold.

The size of perforation was evaluated in a more recent CFD study reported by Lee et al.⁽³⁷⁾. They noted that the cross flow rate, which was the flow through the perforation from the higher flow nasal cavity to the lower flow cavity, accounted for 6 – 10% of total flow rate when the perforation was 15 mm in diameter. The cross flow rate reduced by 10% during inspiration when the perforation was 10 mm in diameter. The reduc-

tion in cross flow was more dramatic (-54% during inspiration) when the perforation was further reduced to 5 mm in diameter. This phenomenon may explain the whistling in some patients, although the authors acknowledged that further studies were required to simulate sound production. It is likely that whistling may be produced when a perforation and septal deviation occur in tandem. This was demonstrated by Grützenmacher et al. when the nasal models were perfused with air⁽³⁴⁾. No sound was produced in a straight centred septum, despite variations in perforation size.

SEPTAL DEVIATION

When CFD modeling of severe septal deviation was compared to a normal healthy nose, several observations were made. Firstly, the main inspiratory airstreams were channeled away from the common meatus toward the floor and roof of the nasal cavity at higher velocity, bypassing the area of deviated septum (Figure 4A)⁽³⁸⁾. Secondly, the area of high kinetic energy at the head of the inferior turbinate was lost (Figure 4B)⁽³⁹⁾. Thirdly, high wall shear stress was noted in the areas of high airflow velocity (Figure 4C). The overall changes in aerodynamics caused an exaggerated pressure difference in the nasopharynx. This may have an adverse effect on the Eustachian tubal orifice, surrounding muscles and mobility of the soft palate, which are common etiological factors for snoring and obstructive sleep apnoea. High wall shear stress levels in abnormal areas may cause desiccation and mucosal damage, thus predisposing to epistaxis.

ATROPHIC RHINITIS

Atrophic rhinitis (AR) is a debilitating condition that is difficult to treat. It can be a result of chronic nasal infection, endocrine disorders or nutritional deficiencies. Most cases are idiopathic however and are common in Asia and the Middle East⁽⁴⁰⁾. The atrophic nasal cavity has a smaller total surface area and wider cross-sectional area than normal⁽⁴¹⁾. The simulated air temperature was 5.6°C lower than normal, confirming the notion that the AR nasal cavity does not condition inspired air adequately. Furthermore, the airstreams flowed mainly through the upper half of the nasal cavity. In the lower half, a low velocity eddy occurred. The increased airflow across the olfactory groove actually results in anosmia due to the atrophic olfactory epithelium and the abnormal airflow in this region. It is likely that the perception of olfaction occurs when whiffs of air traverse the olfactory groove⁽¹¹⁾, instead of constant high volume airflow. The inability to perceive airflow is another common complaint in AR and is due to the redirected airstreams away from the cold receptors on the atrophic septum and inferior turbinate.

Radical inferior turbinate resection is also recognized as an important cause of atrophic rhinitis⁽⁴²⁾. It was not surprising therefore that the airflow patterns following radical inferior turbinate resection^(29,30) closely approximated that of atrophic

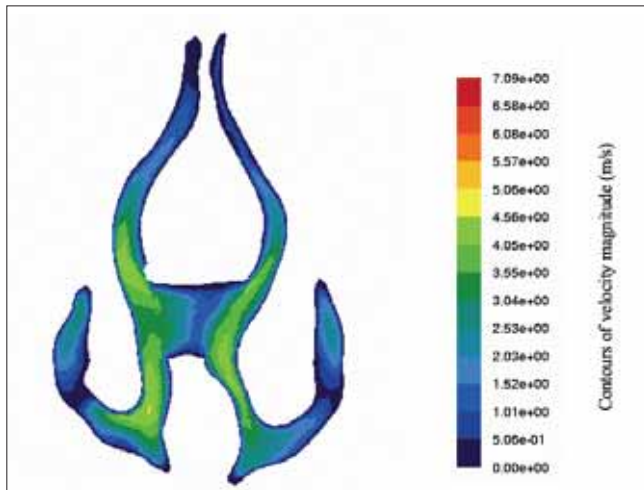


Figure 3. Coronal section across the area of septal perforation illustrating the contours of velocity magnitude.

rhinitis⁽⁴¹⁾. The goal of surgery in AR is to restore the original surface of the nose and to restore the physiological airflow distributions, although achieving these goals remain elusive indeed⁽⁴⁰⁾.

SHORTCOMINGS OF CFD IN CLINICAL RESEARCH

The CFD simulations begin with the acquisition of a geometrical representation of the actual nasal cavity. This is obtained from MRI or CT scans and reconstructed into a three-dimensional computer model (Figure 5) using commercially available software such as Mimics (Materialise, Leuven, Belgium). Thinner scan intervals results in a more accurate reconstructed model. Then, a high-resolution three-dimensional mesh of the nasal cavity is constructed using a variety of software like Hypermesh (HyperWorks, Troy, MI), USA and TGrid (ANSYS Inc., Canonsburg, PA, USA). The resultant model comprised of approximately two million three-dimensional tetrahedral grids where simulations using the commercial computational fluid dynamics code Fluent 6 (Ansys, Inc., Canonsburg, PA, USA) can be performed for each grid. A personal computer (Pentium 4, 2GB RAM) required 28 days per simulation to complete⁽¹¹⁾, although it typically takes about a week for a cluster of networked computers at our institution. It is apparent that CFD simulations require time and high performance computers and as such, is currently unsuitable for use in individual patients.

It can be argued that CFD studies are simulations and the predicted results are derived from complex calculations of the Navier-Stokes equation⁽⁴³⁻⁴⁵⁾, which may not represent real life conditions. In the simulations, air is routinely regarded as being incompressible so that fluid dynamic theories will be applicable. This assumption is acceptable given that the pressure changes within the nasal cavity are small in comparison to the combustion chamber of a jet engine for example. Furthermore, the aerodynamics of nasal airflow is complex due to the geometry of the nasal cavity. Unlike a smooth,

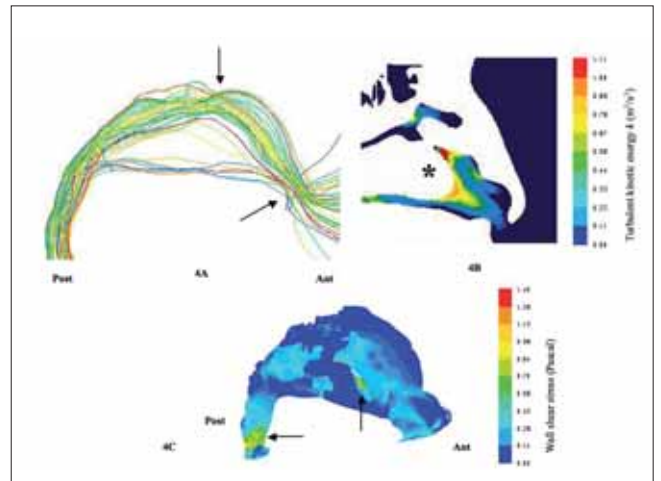


Figure 4. Sagittal view of a nasal cavity with a septal deviation. 4A is the inspiratory airstreams. Arrows point to areas of vortex airflow. Ant = anterior, Post = posterior. 4B is the contour of turbulent kinetic energy κ (m^2/s^2) at the nasal valve region. * = inferior turbinate. 4C is the three-dimensional view of the nasal cavity showing wall shear stress contours. Arrows point to areas of abnormal wall shear stress.

incompressible tube, the nature of nasal airflow (laminar, turbulent or semiturbulent) is not well understood and remains a challenging if not controversial issue⁽⁴⁶⁻⁴⁹⁾. Comparison across CFD studies is also difficult as the presentation of the results is mostly graphical and does not lend to meta-analysis. Although the technical complexities of fluid dynamics are beyond the scope of this review, it is suffice to note that CFD simulations have shown good correlation between the computations and experimental results^(2,50). This suggests that CFD may be a valid method of assessing nasal aerodynamics although more studies are necessary to validate this.

CONCLUSIONS

Unlike other methods of studying nasal airflow such as rhinomanometry and Mink box simulations, CFD technology offers an accurate and highly graphical model to understand the

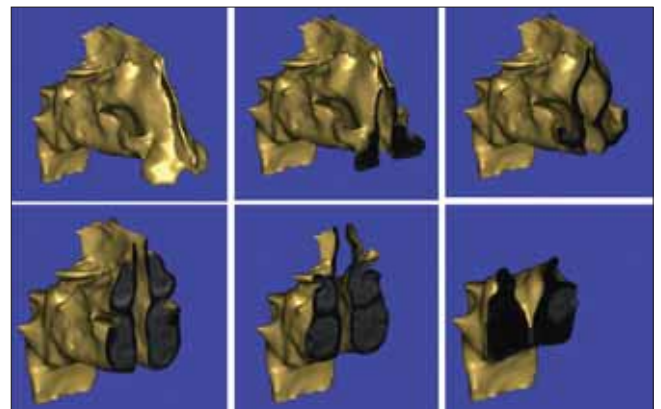


Figure 5. Sequential contour sections of the nasal cavity after three-dimensional reconstruction from MRI or CT scans. These models are used to generate three-dimensional mesh of the nasal airspace to simulate nasal airflow.

nature of nasal aerodynamics. The complex correlations between temperature and humidity, and how these variables affect aerodynamics can also be evaluated. The novel information brought to light by CFD bears serious implications in rhinology. The CFD studies to date have improved our understanding of nasal physiology and offer an explanation of the symptomatology encountered in clinical practice. There is a growing interest in studying the effects of sinonasal surgery on nasal aerodynamics and whether restoration of normal conditions can be achieved. However, many of these studies have performed virtual surgical procedures and will need to be validated with actual post-intervention simulations of real patients. Nonetheless, the importance of preserving mucosa and internal structures such as the turbinates and nasal valve cannot be over emphasized.

Unlike the use of audiometry in hearing loss, there is currently no method of assessing nasal function impairment easily. Despite the numerous studies using rhinomanometry and acoustic rhinometry to study nasal airflow, these tools remain in research laboratories. CFD simulations may be relatively costly and time consuming, it is however conceivable that technology would be available to make CFD a standard tool for rhinologists used in conjunction with other assessments such as imaging and endoscopy⁽⁵¹⁾. Where the diagnosis of some diseases, such as atrophic rhinitis, are on clinical grounds and at the exclusion of other pathologies, individualised CFD studies may be a viable diagnostic tool in the near future. We acknowledge that CFD is not totally infallible, but to date offers an excellent method of studying nasal physiology in health and disease.

ACKNOWLEDGEMENT

The authors would like to acknowledge the financial support by Singapore Ministry of Education Academic Research Tier 2 grant T208A3103. SC Leong is the Rhinology Journal Traveling Fellow 2009/10.

Conflicts of interest: None.

REFERENCES

- Bockholt U, Mlynski G, Müller W, Voss G. Rhinosurgical therapy planning via endonasal airflow simulation. *Comput Aided Surg* 2000; 5: 175-179.
- Doorly DJ, Taylor DJ, Schroter RC. Mechanics of airflow in the human nasal airways. *Respir Physiol Neurobiol* 2008; 163: 100-110.
- Bailie N, Hanna B, Watterson J, Gallagher G. An overview of numerical modelling of nasal airflow. *Rhinology* 2006; 44: 53-57.
- Kimbell JS, Subramaniam RP. Use of computational fluid dynamics models for dosimetry of inhaled gases in the nasal passages. *Inhal Toxicol* 2001; 13: 325-334.
- Suh MW, Jin HR, Kim JH. Computed tomography versus nasal endoscopy for the measurement of the internal nasal valve angle in Asians. *Acta Otolaryngol* 2008; 128: 675-679.
- Terheyden H, Maune S, Mertens J, Hilberg O. Acoustic rhinometry: validation by three-dimensionally reconstructed computer tomographic scans. *J Appl Physiol* 2000; 89: 1013-1021.
- Yu S, Liu Y, Sun X, Li S. Influence of nasal structure on the distribution of airflow in nasal cavity. *Rhinology* 2008; 46: 137-143.
- Haight JS, Cole P. The site and function of the nasal valve. *Laryngoscope* 1983; 93: 49-55.
- Eccles R. Nasal airflow in health and disease. *Acta Otolaryngol* 2000; 120: 580-595.
- Bailie N, Hanna B, Watterson J, Gallagher G. A model of airflow in the nasal cavities: Implications for nasal air conditioning and epistaxis. *Am J Rhinol Allergy* 2009; 23: 244-249.
- Ishikawa S, Nakayama T, Watanabe M, Matsuzawa T. Visualization of flow resistance in physiological nasal respiration: analysis of velocity and vorticities using numerical simulation. *Arch Otolaryngol Head Neck Surg* 2006; 132: 1203-1209.
- Wittkopf M, Wittkopf J, Ries WR. The diagnosis and treatment of nasal valve collapse. *Curr Opin Otolaryngol Head Neck Surg* 2008; 16: 10-13.
- Segal RA, Kepler GM, Kimbell JS. Effects of differences in nasal anatomy on airflow distribution: a comparison of four individuals at rest. *Ann Biomed Eng* 2008; 36: 1870-1882.
- Xiong GX, Zhan JM, Jiang HY, Li JF, Rong LW, Xu G. Computational fluid dynamics simulation of airflow in the normal nasal cavity and paranasal sinuses. *Am J Rhinol* 2008; 22: 477-482.
- Xiong G, Zhan J, Zuo K, Li J, Rong L, Xu G. Numerical flow simulation in the post-endoscopic sinus surgery nasal cavity. *Med Biol Eng Comput* 2008; 46: 1161-1167.
- Ozlugedik S, Nakiboglu G, Sert C, et al. Numerical study of the aerodynamic effects of septoplasty and partial lateral turbinectomy. *Laryngoscope* 2008; 118: 330-334.
- Ishikawa S, Nakayama T, Watanabe M, Matsuzawa T. Flow mechanisms in the human olfactory groove: numerical simulation of nasal physiological respiration during inspiration, expiration, and sniffing. *Arch Otolaryngol Head Neck Surg* 2009; 135: 156-162.
- Lindemann J, Keck T, Wiesmiller K, et al. A numerical simulation of intranasal air temperature during inspiration. *Laryngoscope* 2004; 114: 1037-1041.
- Pless D, Keck T, Wiesmiller K, et al. Numerical simulation of air temperature and airflow patterns in the human nose during expiration. *Clin Otolaryngol Allied Sci* 2004; 29: 642-647.
- Lindemann J, Keck T, Wiesmiller K, et al. Nasal air temperature and airflow during respiration in numerical simulation based on multislice computed tomography scan. *Am J Rhinol* 2006; 20: 219-223.
- Cole P. The four components of the nasal valve. *Am J Rhinol* 2003; 17: 107-110.
- Hanif J, Jawad SS, Eccles R. The nasal cycle in health and disease. *Clin Otolaryngol Allied Sci* 2000; 25: 461-467.
- Egeli E, Demirci L, Yazıcı B, Harputluoglu U. Evaluation of the inferior turbinate in patients with deviated nasal septum by using computed tomography. *Laryngoscope* 2004; 114: 113-117.
- Farmer SE, Eccles R. Chronic inferior turbinate enlargement and the implications for surgical intervention. *Rhinology* 2006; 44: 234-238.
- Lee HP, Poh HJ, Chong FH, Wang DY. Changes of airflow pattern in inferior turbinate hypertrophy: a computational fluid dynamics model. *Am J Rhinol Allergy* 2009; 23: 153-158.
- Eccles R, Jones AS. The effect of menthol on nasal resistance to air flow. *J Laryngol Otol* 1983; 97: 705-709.
- Clement WA, White PS. Trends in turbinate surgery literature: a 35-year review. *Clin Otolaryngol Allied Sci* 2001; 26: 124-128.
- Batra PS, Seiden AM, Smith TL. Surgical management of adult inferior turbinate hypertrophy: a Systematic Review of the Evidence. *Laryngoscope* 2009; 119: 1819-1827.
- Wexler D, Segal R, Kimbell J. Aerodynamic effects of inferior turbinate reduction: computational fluid dynamics simulation. *Arch Otolaryngol Head Neck Surg* 2005; 131: 1102-1107.
- Lindemann J, Keck T, Wiesmiller KM, Rettinger G, Brambs HJ, Pless D. Numerical simulation of intranasal air flow and temperature after resection of the turbinates. *Rhinology* 2005; 43: 24-28.
- Pedroza F, Patrocinio LG, Arevalo O. A review of 25-year experience of nasal septal perforation repair. *Arch Facial Plast Surg* 2007; 9: 12-18.

32. Brain D. Septo-rhinoplasty: the closure of septal perforations. *J Laryngol Otol* 1980; 94: 495-505.
33. Grützenmacher S, Lang C, Saadi R, Mlynski G. First findings about the nasal airflow in noses with septal perforation. *Laryngorhinootologie* 2002; 81: 276-279.
34. Grützenmacher S, Mlynski R, Lang C, Scholz S, Saadi R, Mlynski G. The nasal airflow in noses with septal perforation: a model study. *ORL J Otorhinolaryngol Relat Spec* 2005; 67: 142-147.
35. Grant O, Bailie N, Watterson J, Cole J, Gallagher G, Hanna B. Numerical model of a nasal septal perforation. *Stud Health Technol Inform* 2004; 107: 1352-1356.
36. Pless D, Keck T, Wiesmiller KM, Lamche R, Aschoff AJ, Lindemann J. Numerical simulation of airflow patterns and air temperature distribution during inspiration in a nose model with septal perforation. *Am J Rhinol* 2004; 18: 357-362.
37. Lee HP, Garlapati RR, Chong FH, Wang DY. Effects of septal perforation on nasal airflow – a computer simulation study. *J Laryngol Otol* 2010; 124: 48-54.
38. Zhao K, Pribitkin EA, Cowart BJ, Rosen D, Scherer PW, Dalton P. Numerical modeling of nasal obstruction and endoscopic surgical intervention: outcome to airflow and olfaction. *Am J Rhinol* 2006; 20: 308-316.
39. Chen XB, Lee HP, Hin Chong VF, Wang DY. Assessment of septal deviation effects on nasal air flow: A computational fluid dynamics model. *Laryngoscope* 2009; 119: 1730-1736.
40. Dutt SN, Kameswaran M. The aetiology and management of atrophic rhinitis. *J Laryngol Otol* 2005; 119: 843-852.
41. Garcia GJ, Bailie N, Martins DA, Kimbell JS. Atrophic rhinitis: a CFD study of air conditioning in the nasal cavity. *J Appl Physiol* 2007; 103: 1082-1092.
42. Moore EJ, Kern EB. Atrophic rhinitis: a review of 242 cases. *Am J Rhinol* 2001; 15: 355-361.
43. Batchelor GK. *An Introduction to Fluid Dynamics*, Cambridge University Press, 1967.
44. Petrilu T, Trif D. *Basics of fluid mechanics and introduction to computational fluid dynamics*, New York : Springer, 2005.
45. Chung TJ. *Computational fluid dynamics*, Cambridge University Press, 2002.
46. Liu Y, Edgar AM, Gu JJ, et al., Numerical simulation of aerosol deposition in a 3-D human nasal cavity using RANS, RANS/EIM, and LES. *J Aerosol Sci* 2007; 38: 683-700.
47. Jeong SJ, Kim WS, Sung SJ. Numerical investigation on the flow characteristics and aerodynamic force of the upper airway of patient with obstructive sleep apnea using computational fluid dynamics. *Mech Eng Physics* 2007; 29: 637-651.
48. Li WI, Perzl M, Heyder J, et al., Aerodynamics and aerosol deaggregation phenomena in model oralpharyngeal cavities. *J Aerosol Sci* 1996; 27: 1269-1286.
49. Katz IM, Davis BM, Martonen TB. A numerical study of particle motion within the human larynx and trachea. *J Aerosol Sci* 1999; 30: 173-183.
50. Mylavaparu G, Murugappan S, Mihaescu M, et al. Validation of computational fluid dynamics methodology used for human upper airway flow simulations. *J Biomech* 2009; 42: 1553-1559.
51. Weinhold I, Mlynski G. Numerical simulation of airflow in the human nose. *Eur Arch Otorhinolaryngol* 2004; 261: 452-455.

De Yun Wang, MD PhD
Department of Otolaryngology – Head and neck Surgery
Yong Loo Lin School of Medicine
National University of Singapore
5 Lower Kent Ridge Road
Singapore 119260